BeBeC-2022-D01

HYBRID APPROACH FOR DECONVOLUTING TONAL NOISE OF MOVING SOURCES

Timo Schumacher[1] and Henri Siller[2]
[1]Technische Universität Berlin, ISTA, FG Turbomaschinen- und Thermoakustik
Müller-Breslau-Str. 8, 10623 Berlin, Germany
[2]German Aerospace Center (DLR), Institute of Propulsion Technology, Engine Acoustics Department
Müller-Breslau-Str. 8, 10623 Berlin, Germany

Abstract

For the assessment of noise reduction measures on aircraft and aircraft engines, flyover measurements are necessary to provide a realistic estimation of their effectiveness. The use of microphone arrays improves the ability to localize the sources and quantify the noise levels of different components of the aircraft. The department of Engine Acoustics at the German Aerospace Center uses a hybrid approach, where in the first step, a delay-and-sum beamforming (CBF) is executed in the time-domain followed by a deconvolution, similar to DAMAS, in the frequency domain. While the algorithm used at DLR relies on the assumption of broadband sources, where the loss of energy from one frequency band to neighboring bands can be assumed to equal to the gain from these bands, this may not hold true of tonal sources and requires a new approach. While good results can be achieved with the current approach for practical applications, this paper investigates the feasibility of interconnecting neighboring frequency bands in the deconvolution step and the resulting benefit in the localization of tonal sources from fly-over measurements.

1 INTRODUCTION

This papers aim is to show how an interconnection across frequencies of the deconvolution problems can be accomplished. This makes the deconvolution suitable for tonal sources, which were so far neglected by the hybrid deconvolution method proposed by [4, 6]. For this, we will first derive the point spread function of moving sources across neighboring narrow band frequencies. The presented model will take the properties of the spectral analysis into account without the need of numerically performing a costly fourier transform as in [2]. We will then give an estimate of the computational cost of the deconvolution for the full problem across frequencies and discuss the feasibility of this approach. Further, we want to derive a method using a priori knowledge of the frequencies with tonal components where a limited number of neighboring frequency bands are considered. These methods will be applied to simulations representing flyover measurements.

2 Method

2.1 Beamforming formulation in the time domain

The classical sum-and-delay approach for source localization with phased microphone arrays is a well established method and can be applied both the time and the frequency domain. When using it to focus on a potential source position, the recorded pressure signals $p_m(t)$ at the M microphones are delayed, amplified and averaged to reconstruct the source signal. In general, the content of the microphone signals that does not originate from this source position is suppressed.

While not a requirement to the general approach, the source terms are usually modelled as point sources, often monopoles. They can easily be arranged in a scanning grid. The resulting sound levels at the grid points give an indication of the source distribution.

Forward Model for Moving Sources

In many applications of phased microphone arrays, the classical approach is applied in the frequency domain, where the delay translates to a phase difference. For a time-dependent acoustic source, which includes sources moving along a trajectory $\vec{x}_s(t)$, the delay-and-sum method is typically applied in the time-domain, where the movement can be easily taken into account.

The formulation of the delay-and-sum beamforming serves as the basis of the propagation model for the deconvolution, presented in the following sections. To introduce the notation, a short derivation is provided here.

$Q_s(\tau)$ represents the signal associated with a monopol at position $\vec{x}_s(\tau)$. In this context τ is used to signalize that the position and the signal both are evaluated at emission time.

To express the component of a microphone signal attributed to $Q_s(\tau)$, the Green function for moving monopoles can be used to analytically describe the pressure at a fixed microphone position in the farfield as

$$p_s(\vec{x}_m, t) = \frac{Q_s(\tau_{sm})}{r_{sm}(\tau_{sm})|1 - M_{sm}(\tau_{sm})|}, \tag{1}$$

. where $r_{sm}(\tau) = |\vec{x}_m - \vec{x}_s(\tau)|$ describes the distance between microphone m and source s [3]. The emission time $\tau_{sm} = \tau_{sm}(t)$ is a function of the reception time t and the solution of

$$\tau_{sm} = t - \frac{|\vec{x}_m - \vec{x}_s(\tau_{sm})|}{c} = t - \frac{r_{sm}(\tau_{sm})}{c}. \tag{2}$$

To improve readability, the explicit notation for the time dependency is omitted. For subsonic linear movement, this solution is unique and can be found analytically.

$M_{sm}(\tau)$ is the observer Mach number, which is defined by the projection of a Mach vector towards the microphone position

$$M_{sm}(\tau) = \frac{\langle \vec{x}_m - \vec{x}_s(\tau), \vec{v}_s(\tau) \rangle}{|\vec{x}_m - \vec{x}_s(\tau)|\, c_0} = M\cos(\theta_{sm})\ , \tag{3}$$

with $\vec{v}_s(\tau)$ being the velocity of source s and θ_{sm} is the angle between $\vec{v}_s(\tau)$ and $(\vec{x}_m - \vec{x}_s(\tau))$.
Furthermore, we define

$$T_{sm}(\tau) = \frac{1}{r_{sm}(\tau)|1 - M_{sm}(\tau)|} = \frac{D_{sm}(\tau)}{r_{sm}(\tau)} \tag{4}$$

as the attenuation coefficient due to the propagation and source velocity.

To obtain delay-and-sum beamforming for a given focus point $\vec{x}_f(\tau)$, the delay and attenuation of the given propagation model are inverted for each microphone and then averaged:

$$y^{BF}(\vec{x}_f, \tau) = \sum_{m=1}^{M} w_m T_{mf}^{-1}(\tau) p(\vec{x}_m, t_{mf})\ , \tag{5}$$

where the reception time

$$t_{mf} = t_{mf}(\tau) = \tau + \frac{|\vec{x}_m - \vec{x}_s(\tau)|}{c} \tag{6}$$

is the inverse function of the previously defined function $\tau_{fm}(t)$. w_m are weighting factors for each microphone and add up to one. They can be adjusted depending on the microphone position and the analyzed frequency range. In the easiest case of uniform weighting $w_m = {}^1/_M$ holds true for each microphone.

Spectral Analysis

In most applications, the resulting beamforming signal $y^{BF}(\vec{x}_f, \tau)$ is not examined directly in the time domain but transformed into a frequency spectrum.

For practical purposes, Welch's method can be used [11]. For this, the examined total time interval gets segmented into D subintervals of shorter duration T. The autopower spectrum of each segment is then averaged. Since a reduced interval duration causes a lower frequency resolution, this effectively sacrifices frequency resolution for better statistical properties.

$$Y^{BF}(\vec{x}_f, f_l) := \frac{1}{D}\sum_{d}^{D} \left| \mathscr{F}_\tau \left\{ h_T^{\{d\}}(\tau) y^{BF}(\vec{x}_f, \tau) \right\}(f_l) \right|^2 \tag{7}$$

$$= \frac{1}{D}\sum_{d}^{D} \left| \mathscr{F}_\tau \left\{ h_T^{\{d\}}(\tau) \sum_{m=1}^{M} w_m T_{mf}^{-1}(\tau) p(\vec{x}_m, t_{mf}) \right\}(f_l) \right|^2 . \tag{8}$$

Here $h_T^{\{d\}}(\tau)$ is a window function of width T and centered around $\tau_0^{\{d\}}$, so that $h_T^{\{d\}}(\tau) = 0$ for $\left|\tau - \tau_0^{\{d\}}\right| > {}^T/_2$. This effectively masks the operating space of the Fourier transform to the interval $\tau \in \left[\tau_0^{\{d\}} - \frac{T}{2}, \tau_0^{\{d\}} + \frac{T}{2}\right]$ indexed by d, which is the desired underlying instrument of

Welch's method. The frequency resolution is defined by $\Delta f = {}^{1}/_{T}$. Thus, the frequency-space is discretized to values of $f_l = l\Delta f,\ l = \mathbb{N}$.

While digital signals are discrete in time, a continuous representation is convenient at this point. It is assumed that the signal is bandlimited and sampled with a sufficiently high sampling rate to prevent aliasing.

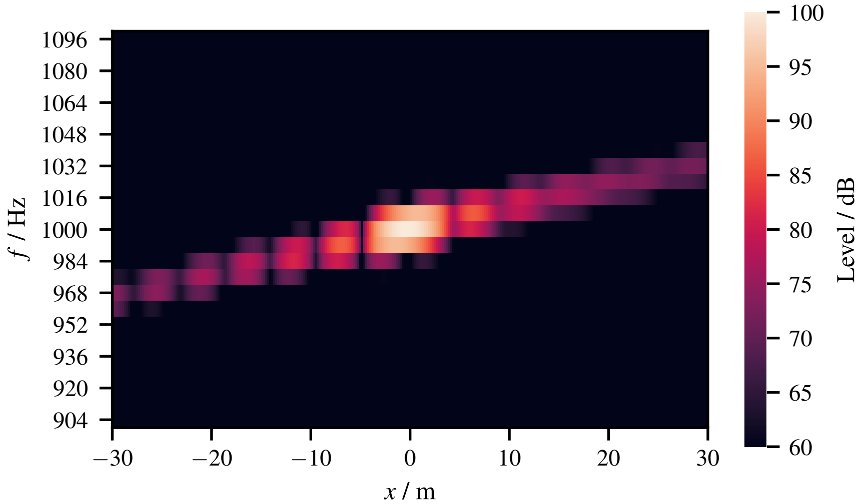

Figure 1: Beamforming results of a monopol at altitude 200 m *and* $v_x = 80\,\mathrm{m/s}$. *The source is a tonal source with* 1 kHz *and* 100 dB. *The line array consists of* 101 *equally spaced microphones, For demonstration purposes, the geometric setup replicates the beamforming pattern in [5].*
The chosen time segment of a total length of 0.88 s *scans the source right over the array, with the emission angle interval ranging from* 80° *to* 100°. *The spectral analysis was done with FFTs of* 13 *overlapping subsegments, each with a length of* 0.125 s, *resulting in a frequency resolution of* $\Delta f = 8\,\mathrm{Hz}$. *The segments where weighted with the Hann window function.*

2.2 Deconvolution Methods

The sum-and-delay approach is robust and well described. However, it does suffer from a limited spatial resolution [7, 8]. It can be easily shown that focusing on a point source $\left(\vec{x}_s(t) = \vec{x}_f(t)\right)$ correctly reconstructs the original signal, as long as no or only weaker sources are in the vicinity. When focusing on positions or trajectories that are not aligned with the real source, the determined power at these positions is generally suppressed but not zero. This effect is referred to as the imaging properties and depends on the geometric setup, the examined frequency and the positions $\vec{x}_s$ and $\vec{x}_f$. It can generally be described as a convolution of the real source strengths with the point-spread-function, which describes the linear impact of source s (with frequency f_k) on the beamforming result at a grid position or focus point f. It leads to a limited resolution of the method. Especially at low frequencies, real sources close to each other can not be separated but appear as one source. Great care must be taken when interpreting sourcemaps of complex source distributions.

An established family of methods for obtaining a higher resolution sourcemap are called deconvolution methods [1, 6]. Taking a model for the point-spread-function, they aim to find a source distribution that closely reproduce the sum-and-delay beamforming results.

Typically, that includes a linear problem of the shape

$$AX = Y \,, \tag{9}$$

where the system-matrix $A \in \mathbb{R}^{F \times S}$ represents the point-spread-function, $Y \in \mathbb{R}^F$ a vector of the sum-and-delay beamforming results for each focus point f and $X \in \mathbb{R}^S$ the unknown source strength. When the same grid is used for computed source strength and the modeled ones, this yields a quadratic system of linear equation that can be solved e.g. iteratively.

It must be noted that the point-spread-function for stationary sources of a given frequeny only re-distributes the power within one frequency band, i.e.

$$\mathrm{PSF}\left(\vec{x}_f, \vec{x}_s; f_l, f_k\right) = 0 \quad \text{for}\, f_l \neq f_k \,. \tag{10}$$

This enables the computation of the deconvolution separately for each frequency band, as described in eq. (9).

However eq. (10) is not true for moving sources however. The frequency shift due to the Doppler effect is improperly corrected when scanning the grid on positions away from the real source distribution. This causes a shift in frequency, depending on the source and trajection of the focus point (see Fig. 1).

Different schemes have been proposed to address this. Guérin and Weckmüller [6] introduced a hybrid scheme for moving sources, where the beamforming and spectral analysis are executed as described in section 2.1. Furthermore they argue, that this error can be neglected for broadband sources. This approach has successfully been the base of several applications of flyover measurements [4, 9, 10]. When applying this scheme to tonal sources, it can neither correctly locate the source in space nor in frequency (see Fig. 2). Some following works considering the effect of the movement on point spread functions have been added by the authors [5].

More recently [2] proposed a deconvolution that takes the point-spread-function across frequencies into account. For the calculation, repeated FFTs are necessary, which come with a significant computational cost.

2.3 A New Propagation Model for Moving Sources

The proposed approach takes not just the array geometry and source positions into account, but also considers the properties of the next elements of the process chain. It does so without costly Fourier transform by a analytic evaluation of the windows used for the spectral analysis.

For the derivation of the point-spread-function, we model a source at position $\vec{x}_s(t)$ as a sum of discrete, equally spaced frequency components $f_k = k\Delta f^k/T, k \in \{1, ..., K\}$

$$Q_s(\tau) = \sum_k^K A_{s;k} e^{j2\pi f_k \tau} \,. \tag{11}$$

The amplitude $A_{s;k}$ is the amplitude of source $s \in \{1, ..., S\}$ at frequency f_k. The microphone

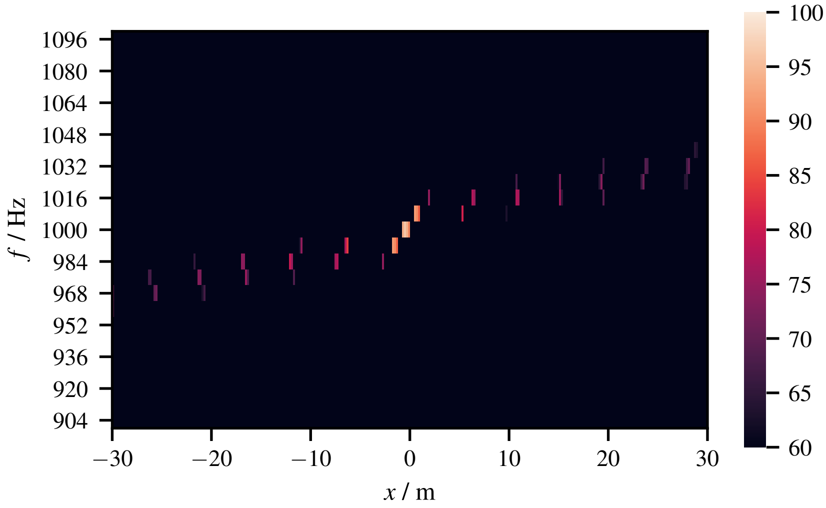

Figure 2: Results of the hybrid deconvolution as described by [6] results of the simulated source of Fig. 1. As this deconvolution does not consider the interconnection of frequencies, it is unable to resolve them and correctly locate the tonal source, both in space and frequency. The amplitude at $x = 0\,\mathrm{m}$ *and* $f = 1000\,\mathrm{Hz}$ *is underestimated with* 96.2 dB.

signal $p\left(\vec{x}_m, t\right)$ is the sum of the propagated signals of all sources, defined in eq. (1).

$$p(\vec{x}_m, t) = \sum_{s}^{S} p_s(\vec{x}_m, t) = \sum_{s}^{S} T_{sm}(\tau_s m) \sum_{k}^{K} A_{s;k} e^{j2\pi f_k \tau_{sm}} \,, \tag{12}$$

Inserting eq. (12) into eq. (5) yields the time-domain beamforming definition

$$\begin{aligned} y^{BF}\left(\vec{x}_f, \tau\right) &= \sum_{m=1}^{M} w_m T_{mf}^{-1}(\tau) \sum_{s=1}^{S} T_{sm}(\tau_{sm}) \sum_{k=1}^{K} A_{s;f_k} e^{j2\pi f_k \tau_{sm}} \\ &= \sum_{s=1}^{S} \sum_{k=1}^{K} \sum_{m=1}^{M} w_m \frac{T_{sm}(\tau_{sm})}{T_{mf}(\tau)} A_{s;f_k} e^{j2\pi f_k \tau_{sm}} \,, \end{aligned} \tag{13}$$

where $\tau_{sm} = \tau_{sm}\left(t_{mf}(\tau)\right)$, with τ being the emission time at the focus point and τ_{sm} being the emission time at the assumed source.

$$\begin{aligned} Y_{f;l}^{BF} &= \frac{1}{D} \sum_{d}^{D} \left| \mathscr{F}_\tau \left\{ h^{\{d\}}(\tau) y^{BF}\left(\vec{x}_f, \tau\right) \right\} (f_l) \right|^2 \\ &= \frac{1}{D} \sum_{d}^{D} \left| \sum_{s=1}^{S} \sum_{k=1}^{K} \sum_{m=1}^{M} w_m A_{s;f_k} \mathscr{F}_\tau \left\{ h^{\{d\}}(\tau) \frac{T_{sm}(\tau_{sm})}{T_{mf}(\tau)} e^{j2\pi f_k \tau_{sm}} \right\} (f_l) \right|^2 \end{aligned} \tag{14}$$

To motivate a linear relation between the power $\left|A_{s;f_k}\right|^2$ of each frequency component and the resulting spectra at the focus points $Y^{BF}(\vec{x}_f, f_l) = Y^{BF}_{f;l}$, the sources are assumed to be mutually incoherent. This allows rewriting eq. (14) as

$$Y^{BF}_{f;l} = \sum_s^S \sum_k^K |A_{s;f_k}|^2 \cdot \frac{1}{D} \sum_d^D \left| \sum_m^M \frac{T_{sm}}{T_{fm}} \mathscr{F}_\tau \left\{ h_T^{\{d\}}(\tau) e^{j2\pi f_k \tau_{sm}} \right\} (f_l) \right|^2 = \sum_s^S \sum_k^K |A_{s;f_k}|^2 PSF_{fs;f_l f_k} . \tag{15}$$

This shows the desired factor to be

$$\mathrm{PSF}_{fs;lk} = \frac{1}{D} \sum_d^D \left| \sum_m^M \frac{T_{sm}}{T_{fm}} \mathscr{F}_\tau \left\{ h_T^{\{d\}}(\tau) e^{j2\pi f_k \tau_{sm}} \right\} (f_l) \right|^2 . \tag{16}$$

Because of the dependency $\tau_{sm} = \tau_{sm}\left(t_{mf}(\tau)\right)$, caution must be taken when evaluation the Fourier term. To avoid a costly numeric evaluation of the Fourier transform, one can make some approximations, starting with expressing τ_{sm} as a Taylor Series of second degree

$$\tau_{sm}\left(t_{mf}(\tau)\right) \approx \tau_{sm}\left(t_{mf}\left(\tau_0^{\{d\}}\right)\right) + \left(\tau - \tau_0^{\{d\}}\right) \frac{\partial \tau_{sm}}{\partial t_{mf}} \frac{\partial t_{mf}}{\partial \tau} , \tag{17}$$

centered around $\tau_0^{\{d\}}$ for each interval. Both terms can be efficiently approximated, the first being

$$\begin{aligned} \tau_{sm}\left(t_{mf}\left(\tau_0^{\{d\}}\right)\right) &= \tau_0^{\{d\}} + \frac{r_{fm}\left(\tau_0^{\{d\}}\right) - r_{sm}(\tau_{sm})}{c} \\ &\approx \tau_0^{\{d\}} + D_{fm}\left(\tau_0^{\{d\}}\right) \frac{r_{fm} - r_{sm}}{c} , \end{aligned} \tag{18}$$

the composite derivative as

$$\frac{\partial \tau_{sm}}{\partial \tau}\left(\tau_0^{\{d\}}\right) = \frac{\partial \tau_{sm}}{\partial t_{mf}} \frac{\partial t_{mf}}{\partial \tau}\left(\tau_0^{\{d\}}\right) \approx \frac{1 - M_{fm}}{1 - M_{sm}} = \frac{D_{sm}}{D_{fm}} . \tag{19}$$

If no explicit emission time is indicated, the values are evaluated at $\tau_0^{\{d\}}$, i.e. $r_{fm} = r_{fm}\left(\tau_0^{\{d\}}\right)$.

This allows the definition of a phase difference

$$\varphi^{\{d\}}_{fsm;k} = 2\pi f_k D_{fm} \frac{r_{fm} - r_{sm}}{c} \tag{20}$$

and a instantaneous frequency

$$\hat{f}^{\{d\}}_{fsm;k} = f_k \frac{D_{sm}}{D_{fm}} \tag{21}$$

due to the Doppler effect. Evaluating the Fourier transform results in a convolution of the window function in the frequency domain. As the Fourier transform of the approximated signal contains only the doppler shifted frequency, the convolution can be easily determined:

$$\mathscr{F}_\tau\left\{h_T^{\{d\}}(\tau)e^{j2\pi f_k \tau_{sm}}\right\}(f_l) \approx e^{j\varphi^{\{d\}}_{fsm;k}}\mathscr{F}_\tau\left\{h_T^{\{d\}}(\tau)e^{j2\pi\hat{f}^{\{d\}}_{fsm;k}}\right\}(f_l) \tag{22}$$

$$= e^{j\varphi^{\{d\}}_{fsm;k}} H_T^{\{d\}}(f_k) * \delta\left(f_l - \hat{f}^{\{d\}}_{fsm;k}\right) \tag{23}$$

$$= e^{j\varphi^{\{d\}}_{fsm;k}} H_T^{\{d\}}\left(f_l - \hat{f}^{\{d\}}_{fsm;k}\right) \tag{24}$$

This yields the modeled PSF as

$$\boxed{\mathrm{PSF}_{fs;lk} := \frac{1}{D}\sum_d^D \left|\sum_m^M \frac{T_{sm}}{T_{fm}} e^{j\varphi^{\{d\}}_{fsm;k}} H_T^{\{d\}}\left(f_l - \hat{f}^{\{d\}}_{fsm;k}\right)\right|^2} \tag{25}$$

and the underlying linear system of equations

$$\sum_s^S \sum_k^K \mathrm{PSF}_{fs;lk} X_{s;k} = Y^{BF}_{f;l} \ , \tag{26}$$

which can be easily rearranged into a system matrix and column vectors.

3 Application to flyover measurement data

When solving the linear system of eq. (26) for a scanning grid with high spatial resolution and all available frequencies, limits of computational feasibility can quickly be reached. The number of elements of the point spread function increases quadratically with both the number of considered frequencies and the number of grid points. Assuming the grid contains 10000 points and the frequency range goes up to 8000 Hz (with $\Delta f = 8$ Hz), $\mathrm{PSF}_{fs;lk}$ contains 1.6×10^{15} elements. This number is too high to handle computationally, let alone solve for $X_{s;k}$. We propose an a priori approach, where at first knowledge about the tonal sources is collected with a deconvolution per frequency. The deconvolution across multiple frequencies can be greatly reduced when applied only to neighboring bands of the expected tonal source. A coarse evaluation of the point-spread-function can then be used to determine the band width to consider.

This method was chosen in Fig. 5. Inspecting the modeled point spread function (Fig. 4) shows little to no effect outside the frequency range of 900 Hz to 1100 Hz. The deconvolution of this deliberately simple example with 301 points and 25 spectral lines was computed eas-

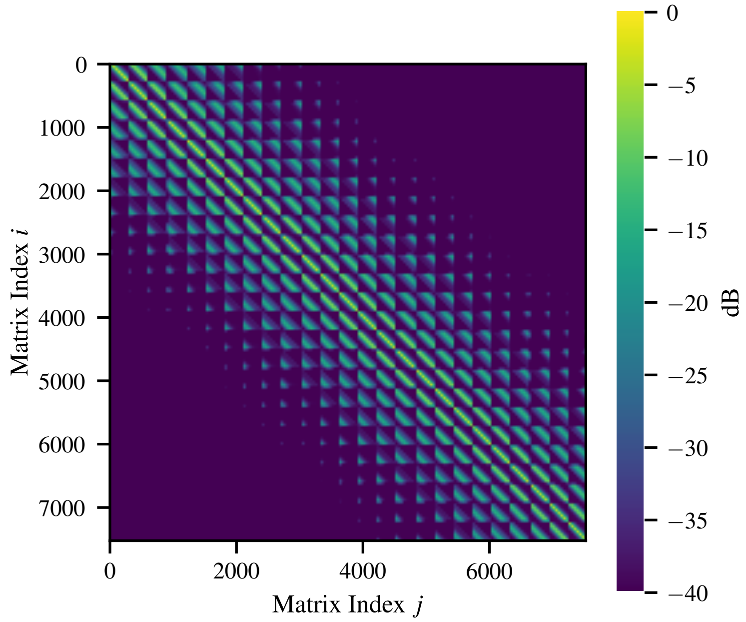

Figure 3: The new system matrix of the deconvolution problem calculated with eq. (25)*. The setup corresponds to the flyover described by Fig. 1. Each block represents a frequency pair f_s, f_f, with $f_s = f_f$ on the diagonal. The displayed frequencies range from* 904 Hz *to* 196 Hz*.*

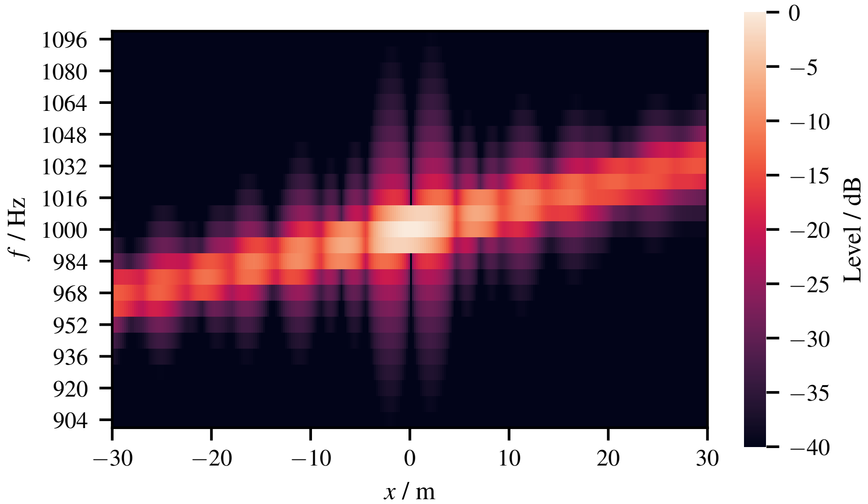

Figure 4: The modeled point spread function of a single virtual source located at the center of the grid, with $f_s = 1000$ Hz. The values in this plot represent a single column in the system matrix (Fig. 3).

ily. 56 625 625 elements of the point spread function had to be computed and were taken into account for solving eq. (26).

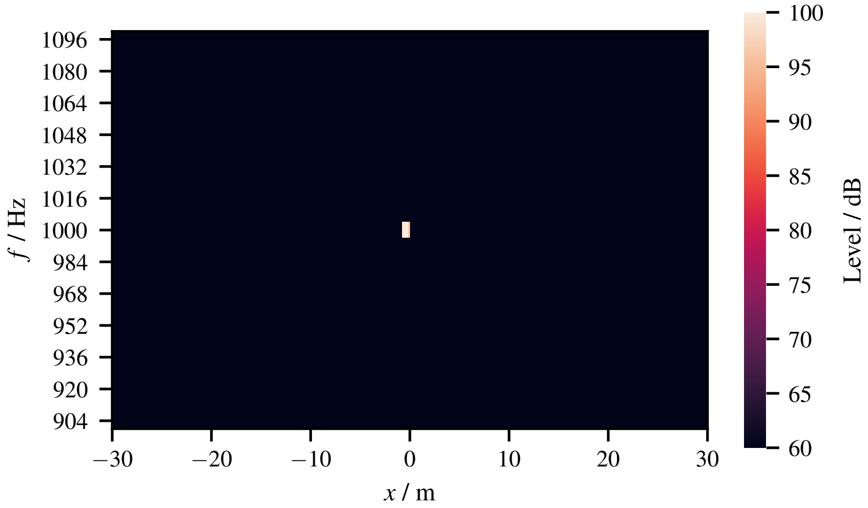

Figure 5: The results of the deconvolution using the new propagation model. The system matrix of Fig. 3 was used. The frequency range considered in the deconvolution was 904 Hz *to* 196 Hz*. The computed level at the center point at* 1000 Hz *is* 99 dB.

4 Conclusion

In this contribution, a new propagation model for the deconvolution of moving tonal sources has been presented. Based on previous works by Guérin and Weckmüller[5], the new model also takes the spectral analysis into account. By including this essential processing step of the delay-and-sum beamforming, the new model promises to more accurately predict source positions and strengths on the beamforming map. The method was comprehensibly derived and simplifications and assumptions were depicted when used.

Limits of the interconnection of the deconvolution approach across the whole spectrum were discussed. A simple simulation and successful application demonstrate the general feasibility when the tonal components of the sourcemap are contained within a limited bandwidth.

We aim to further research the capability of the model for use with real fly-over measurement data. A focus will be on the ability to separate closely distributed tonal sources and the robustness of the method.

References

[1] T. F. Brooks and W. M. Humphreys, Jr. "A Deconvolution Approach for the Mapping of Acoustic Sources (DAMAS) Determined from Phased Microphone Arrays." In *10th*

AIAA/CEAS Aeroacoustics Conference, Manchester, Great Britain, May 10-12, 2004. 2004.

[2] N. Chu, Q. Huang, L. Yu, Y. Ning, and D. Wu. "Rotating acoustic source localization: A power propagation forward model and its high-resolution inverse methods." *Measurement*, 174, 109006, 2021. ISSN 02632241. doi:10.1016/j.measurement.2021.109006.

[3] K. Ehrenfried. *Skript zur Vorlesung Strömungsakustik I und II*. Technische Universität Berlin, 2003.

[4] S. Guérin and H. Siller. "A Hybrid Time-Frequency Approach for the Source Localization Analysis of Acoustic Fly-over Tests." In *14th CEAS/AIAA Aeroacoustics Conference, Vancouver, British Columbia, Canada, 5-7 May 2008*. 2008.

[5] S. Guérin and C. Weckmüller. "Frequency-domain reconstruction of the point-spread function for moving sources." In *Proceedings on CD of the 2nd Berlin Beamforming Conference, 19-20 February, 2008*. GFaI, Gesellschaft zu Förderung angewandter Informatik e.V., Berlin, 2008. ISBN 978-3-00-023849-9. URL http://www.bebec.eu/Downloads/BeBeC2008/Papers/BeBeC-2008-14_Guerin_Weckmueller.pdf.

[6] S. Guérin, C. Weckmüller, and U. Michel. "Beamforming and deconvolution for aerodynamic sound sources in motion." In *Proceedings on CD of the 1st Berlin Beamforming Conference, 22–23 November, 2006*. GFaI, Gesellschaft zu Förderung angewandter Informatik e.V., Berlin, 2006. ISBN 978-3-00-019998-1. URL http://www.bebec.eu/Downloads/BeBeC2006/Papers/BeBeC-2006-16_Guerin_Weckmueller_Michel.pdf.

[7] R. Merino-Martínez, P. Sijtsma, M. Snellen, T. Ahlefeldt, J. Antoni, C. J. Bahr, D. Blacodon, D. Ernst, A. Finez, S. Funke, T. F. Geyer, S. Haxter, G. Herold, X. Huang, W. M. Humphreys, Q. Leclère, A. Malgoezar, U. Michel, T. Padois, A. Pereira, C. Picard, E. Sarradj, H. Siller, D. G. Simons, and C. Spehr. "A review of acoustic imaging methods using phased microphone arrays." *CEAS Aeronautical Journal*, 10(1), 197–230, 2019.

[8] M. Möser. *Messtechnik der Akustik*. Springer, 2010.

[9] H. Siller, M. Drescher, G. Saueressig, and R. Lange. "Fly-over source localisation on a Boeing 747-400." In *Proceedings on CD of the 3rd Berlin Beamforming Conference, 24-25 February, 2010*. 2010. URL http://bebec.eu/Downloads/BeBeC2010/Papers/BeBeC-2010-13.pdf.

[10] H. Siller, T. Schumacher, and W. Hage. "Low noise ATRA - phased array measurements of jet noise in flight." *AIAA J.*, 2021. doi:10.2514/6.2021-2160.vid. URL https://doi.org/10.2514/6.2021-2160.vid.

[11] P. Welch. "The use of fast fourier transform for the estimation of power spectra: A method based on time averaging over short, modified periodograms." *IEEE Transactions on Audio and Electroacoustics*, 15(2), 70–73, 1967. doi:10.1109/TAU.1967.1161901.